

## Syntheses and characterization of a series of oxalalix[4]arene-linked cofacial bisporphyrins

Lijuan Jiao<sup>\*a</sup>, Yanhua Fang<sup>b</sup>, Yunyou Zhou<sup>\*b</sup>, Sufan Wang<sup>a</sup>, Erhong Hao<sup>a</sup> and M. Graça H. Vicente<sup>\*c</sup>

<sup>a</sup> Anhui Key Laboratory of Functional Molecular Solids and Anhui Key Laboratory of Molecular Based Materials, College of Chemistry and Material Science, Anhui Normal University, Wuhu, Anhui 241000, China

<sup>b</sup> Anhui Key Laboratory of Chemo-Biosensing, College of Chemistry and Materials Science, Anhui Normal University, Wuhu 241000, China

<sup>c</sup> Department of Chemistry, Louisiana State University, Baton Rouge, LA 70803, USA

Received 22 January 2010

Accepted 6 April 2010

**ABSTRACT:** A series of oxalalix[4]arene-linked cofacial bisporphyrins **2–4** have been synthesized as free-bases, biszinc(II) and biscopper(II) complexes. UV-vis, fluorescence and cyclic voltammetric studies were performed on the bisporphyrins. Little electronic interactions between the two porphyrin macrocycles in both the metal-free and biszinc(II) complexes **2** and **3** were observed, while enhanced electronic communications were observed in the case of **4** bearing two copper(II) metal ions. Geometry optimizations were carried out using HF/CEP-31G methods to investigate the molecular structures of these bisporphyrins. Solvent effects on the photophysical properties of these bisporphyrins are also discussed.

**KEYWORDS:** oxalalix[4]arene, cofacial bisporphyrins, photophysical, cyclic voltammograms.

### INTRODUCTION

Cofacial bisporphyrins play important roles in diverse fields, as light-harvesting devices [1], energy and electron transfer materials [2], and as catalysts for multi-electron redox catalysis [3]. Among these, rigid spacer-linked cofacial bisporphyrins, known as Pacman porphyrins, have been mostly studied as hosts for small-molecule reactions [4]. Most often, Pacman porphyrins [5, 6], such as DPA (diporphyrin anthracene) [7], DPB (diporphyrin biphenylene) [8], DPX (diporphyrin dimethylxanthene) [9], DPD (diporphyrin dibenzofuran) [10] and DPS (diporphyrin dibenzothiophene) [11] are linked by rigid spacers [7–11] including anthracene, biphenylene, dimethylxanthene, dibenzofuran and dibenzothiophene units.

Calixarenes have been extensively studied in the past decade due to their unique conformational cavity structure and their molecular recognition properties. Porphyrin-calix[4]arene conjugates have been synthesized by several groups [12]. Most of these molecules were synthesized *via* the modification of the calixarene fragment. The total synthesis of these porphyrin-calixarene conjugates suffers from long synthetic routes and very low yields. The efficient synthesis of these bisporphyrins remains a challenge, as well as the investigation of their properties [13]. Oxalalix[4]arene is a versatile platform that can be easily functionalized. In addition, this platform has a rigid discrete 1,3-alternate conformation with appreciable flexibility [14] that is limited to a unique form designated “slipped dimer” rather than a “face-to-face dimer” [15].

Attracted to the interesting conformations of this oxalalix[4]arene platform and based on the recent improved synthetic route of this fragment by Katz *et al.* [14a], we have recently reported the synthesis and characterization of a series of oxalalix[n]arene-locked cofacial

<sup>◇</sup>SPP full member in good standing

\*Correspondence to: Lijuan Jiao, email: jiao421@mail.ahnu.edu.cn; Yunyou Zhou, email: zy161299@mail.ahnu.edu.cn and M. Graça H. Vicente, email: vicente@lsu.edu

bisporphyrins and higher oligomers [16]. The X-ray structure of a metal-free bisporphyrin shows a “slipped dimer” conformation [16]. We envisioned that the introduction of metal ions into the porphyrin macrocycles to build the corresponding homobimetallic bisporphyrins would lead to interesting photophysical and electrochemical properties for this system. Herein, we report the synthesis, photophysical and electrochemical properties as well as the geometry optimization based on HF/CEP-31G methods of these new bimetallic oxacalix[4] arene-linked cofacial bisporphyrins **3** and **4** and compare them to those of the previously reported [16] metal-free system **2**.

## EXPERIMENTAL

### General

Reagents were purchased as reagent-grade and used without further purification unless otherwise stated. Solvents were used as received from commercial suppliers unless noted otherwise. THF was freshly distilled from sodium benzophenone ketyl. All reactions were performed in oven-dried or flame-dried glassware unless otherwise stated, and were monitored by TLC using 0.25 mm silica gel plates with UV indicator (60F-254).  $^1\text{H}$  NMR are obtained on a Bruker AV-300 spectrometer at 298 K. Chemical shifts ( $\delta$ ) for  $^1\text{H}$  NMR spectra are given in ppm relative to THF- $d_8$  (3.58 and 1.73 ppm). Chemical shift multiplicities are reported as s = singlet, d = doublet, q = quartet, and m = multiplet. Mass spectra were obtained on an Applied Biosystems QSTAR XL; the matrix used for the MALDI analyses was anthracene. Elemental analysis was obtained on VarioEL III. 5,15-di(3,5-dihydroxyphenyl)porphyrin **1** and oxacalix[4]arene bisporphyrin **2** were synthesized following previously reported procedures [16, 17]. The optimized structures of bisporphyrins **2**, **3** and **4** were modeled by *ab initio* HF/CEP-31G method [18]. The geometrical structure of bisporphyrin **2** was in consistence with its X-ray structure [16].

### Synthesis

**Bis(zinc(II)porphyrin 3** was synthesized by reacting **2** (81 mg, 0.05 mmol) with excess amount of  $\text{Zn}(\text{OAc})_2$  (92 mg, 0.5 mmol) in a refluxing mixture of chloroform/methanol (60 mL, v/v = 3/1). The crude product was purified by column chromatography (silica gel, dichloromethane) to give complex **3** in quantitative yield (87 mg).  $^1\text{H}$  NMR (300 MHz; THF- $d_8$ ):  $\delta_{\text{H}}$ , ppm 9.06 (s, 2H), 8.71 (br, 16H), 8.41 (m, 8H), 8.23 (m, 8H), 7.83 (s, 2H), 7.78 (m, 18H), 7.11 (s, 2H). Anal. calcd. for  $\text{C}_{100}\text{H}_{56}\text{N}_{12}\text{O}_{12}\text{Zn}_2 \cdot 2\text{CH}_3\text{OH}$ : C, 67.59; H, 3.56; N, 9.28%. Found: C, 67.65; H, 3.61; N, 9.14. HRMS (MALDI-TOF):  $m/z$  1748.2728 (calcd. for  $\text{C}_{100}\text{H}_{56}\text{Zn}_2\text{N}_{12}\text{O}_{12}$  1748.2715).

**Bis(copper(II)porphyrin 4**. To a solution of **2** (73 mg, 0.045 mmol) in 50 mL of chloroform was added

$\text{Cu}(\text{OAc})_2 \cdot 2\text{H}_2\text{O}$  (100 mg, 0.45 mmol) in 15 mL of methanol. The resulting solution was refluxed until TLC indicated that the reaction was completed. After removal of the solvents under vacuum, the resulting solid was dissolved in a 1:1 mixture of dichloromethane and water (100 mL). The organic layer was washed with water (3  $\times$  50 mL) and dried over anhydrous  $\text{Na}_2\text{SO}_4$ ; solvent was removed under vacuum. The crude product was purified by column chromatography on silica gel using dichloromethane for elution. Complex **4** was obtained in 90% yield (71 mg). Anal. calcd. for  $\text{C}_{100}\text{H}_{56}\text{Cu}_2\text{N}_{12}\text{O}_{12}$ : C, 68.84; H, 3.24; N, 9.63%. Found: C, 68.70; H, 3.44; N, 9.52. MS (MALDI-TOF):  $m/z$  1744.9 (calcd. for  $\text{C}_{100}\text{H}_{56}\text{Cu}_2\text{N}_{12}\text{O}_{12}$  1744.7).

### Cyclic voltammetry

Cyclic voltammetry (CV) was conducted in a standard three-electrode cell with the use of CHI 660 potentiostat-galvanostat (Shanghai Chenhua Instrumental Cooperation Ltd., China). A Pt wire served as the auxiliary electrode, an Ag/AgCl electrode was used as a reference electrode, and the glassy carbon electrode (GCE) was used as a working electrode. The reference electrode was separated from the bulk of the solution by a bridge filled with the solution to be investigated. The bridge was then placed in another tube ending in a lugging capillary tip. The GC electrode (GCE) was polished consecutively with diamond paste until a mirror finish was obtained. The polished electrode was cleaned in an ultrasonic water bath for 5 min to remove the diamond and carbon particles. The total volume of the electrolysis cell was 2–5 mL and concentrations of porphyrins and bisporphyrins solutions were  $1 \times 10^{-3}$  M. Sweep rate was set at 60  $\text{mV} \cdot \text{s}^{-1}$ . Constant-potential coulometry was conducted at room temperature in dry dichloromethane. Trihexyl(tetradecyl) phosphonium hexafluorophosphate was used as the supporting electrolyte at a concentration of 0.1 M. Deaeration of the solution with high-quality purified nitrogen was performed before commencing the experiment. All experiments were carried out in a controlled temperature room and potentials are reported with respect to the Ag/AgCl electrode.

### UV-vis and fluorescence analysis

UV-visible absorption spectra were recorded on a Hitachi U-3010 spectrophotometer (190–1100 nm scan range). Fluorescence emission spectra were recorded on a Hitachi F-4600 FL spectrophotometer. The slit widths were 2.5 nm and 5.0 nm for excitation and emission, respectively. Solvents and reagent for photophysical studies were purchased as analytical grade and were used freshly distilled. All measurements were recorded at 20 °C. Fluorescence lifetimes were measured on a combined steady-state lifetime fluorescence spectrometer model FLS920 (Edinburgh Instruments) and the fluorescence lifetimes were obtained from deconvolution

and distribution lifetime analysis [19]. Fluorescent quantum yields were calculated using a secondary standard method by comparing the areas under the corrected emission spectrum of the test sample in various solvents with that of the standard. Dilute solutions ( $0.01 < A < 0.05$ ) were used to minimize the reabsorption effects and correction for the solvent refractive index was applied. H<sub>2</sub>TPP in dry DMF ( $\Phi_F = 0.11$  [20]) and ZnTPP in toluene ( $\Phi_F = 0.03$  [21]) were used as a fluorescence standard for the fluorescent quantum yield calculation according to the absorption of the test sample [22]. Quantum yields were determined using the following equation [23]:

$$\Phi_X = \Phi_S (I_X/I_S) (A_S/A_X) (\eta_X/\eta_S) \quad (1)$$

where  $\Phi_S$  stands for the reported quantum yield of the standard,  $I$  stands for the integrated emission spectra,  $A$  stands for the absorbance at the excitation wavelength, and  $\eta$  stands for the refractive index of the solvent being used ( $\eta = 1$  when the same solvent was used for both the test sample and the standard).  $X$  subscript stands for the test sample and  $S$  subscript stands for the standard.

## RESULTS AND DISCUSSION

Metal-free bisporphyrin **2** with a “slipped dimer” conformation (Fig. 1) was synthesized in 91% yield

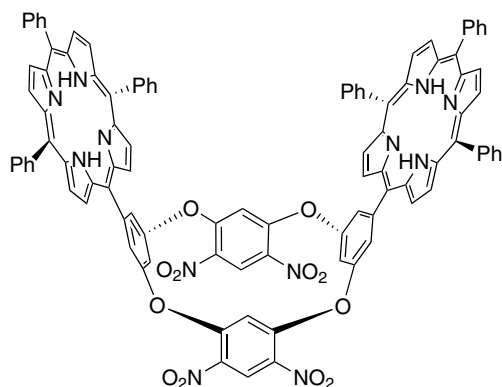
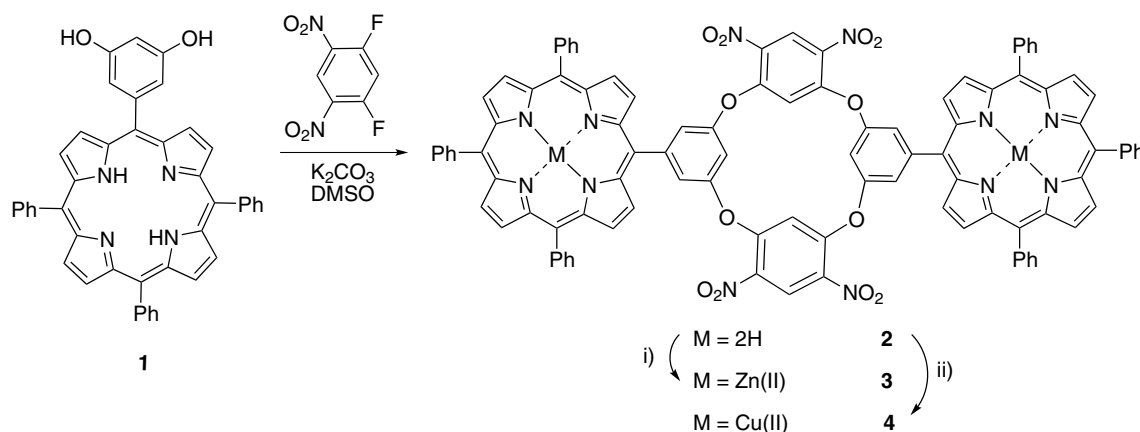


Fig. 1. “Slipped dimer” conformation of bisporphyrin **2**



Scheme 1. Synthesis of oxacalix[4]arene linked cofacial bisporphyrins **2**, **3** and **4**, reaction conditions: (i) excess Zn(OAc)<sub>2</sub>, chloroform/methanol ( $v/v = 3/1$ ), refluxing; (ii) excess Cu(OAc)<sub>2</sub>·2H<sub>2</sub>O, chloroform/methanol ( $v/v = 3/1$ ), refluxing

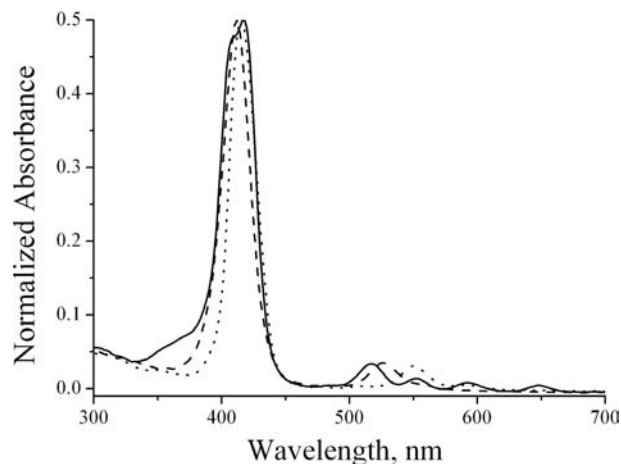
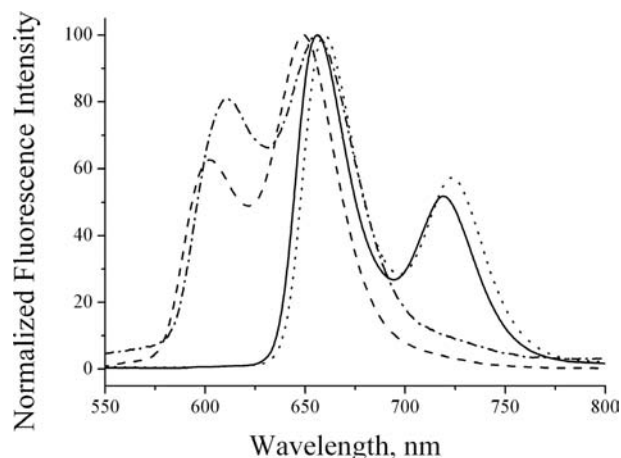
upon reaction of porphyrin **1** with 1,5-difluoro-2,4-dinitrobenzene, as we have previously reported [16]. The starting porphyrin **1** can be prepared in multigram scale by a mixed aldehyde condensation in propionic acid, followed by demethylation with BBr<sub>3</sub> in dichloromethane [17]. The homobimetallic coordination complexes **3** and **4** were prepared by direct reaction of **2** with the corresponding metal(II) salts (as shown in Scheme 1). Complex **3** was synthesized in quantitative yield from the reaction of **2** with Zn(OAc)<sub>2</sub> in a methanol/chloroform mixture and was characterized by <sup>1</sup>H NMR, high-resolution mass spectrometry, and elemental analyses. Complex **4** was obtained in excellent yield (90%) by reaction of **2** with Cu(OAc)<sub>2</sub>·2H<sub>2</sub>O in a methanol/chloroform mixture and was characterized by mass spectra and elemental analysis.

The UV-vis data for bisporphyrins **2**, **3** and **4** at room temperature are presented in Table 1 and Fig. 2. The absorption bands in the Soret and Q regions exhibit the expected patterns for the corresponding two porphyrin chromophores (free-base for **2** or metallic for **3** and **4**). The absorption characteristics of **2** and **3** closely approximate the monomer H<sub>2</sub>TPP and ZnTPP, respectively, indicating the enlarged distance between the two porphyrin chromophores in the “slipped dimer” conformer. In comparison to **2**, little variation in the  $\lambda_{\max}$  of the Soret band was observed for **3**. The two Q bands typical of a metalloporphyrin were observed for **3**, in contrast with those observed for **2**. Therefore, we conclude that the insertion of zinc(II) has little effect on the electronic communication between the two porphyrin macrocycles. The increased separation decreases  $\pi$ - $\pi$  overlap and excitonic coupling between the porphyrin subunits [24]. In contrast, characteristics of strongly interacting porphyrin sub-units was observed in **4**: the blue shift of the Soret band to 412 nm, and the red shift (by 8 nm) of Q(1,0) and the Q(0,0) maxima. These results suggest enhanced excitonic interactions with the insertion of copper(II) ions [25].

The fluorescence data for bisporphyrins **2** and **3** are presented in Table 1 and Fig. 3. The comparison of the

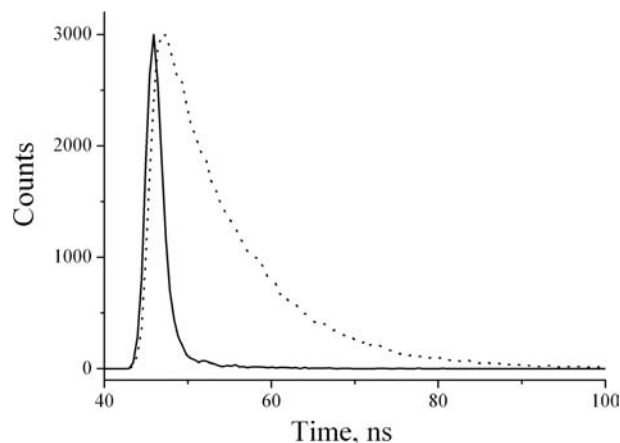
**Table 1.** UV-vis and fluorescence data for bisporphyrins **2**, **3** and **4** in dichloromethane at 20 °C

Compound	log $\epsilon$	$\lambda_{\text{max}}^{\text{abs}}$ , nm		$\lambda_{\text{max}}^{\text{em}}$ , nm	$\Phi_{\text{F}}$	Lifetime $\lambda_{\text{F}}$ , ns ( $\chi^2$ )
		Soret band	Q bands			
H <sub>2</sub> TPP	5.34	417	514, 547, 592, 648	656, 720	0.13	8.47 (1.00)
ZnTPP	5.67	422	550, 590	602, 650	0.04	1.70 (1.01)
<b>2</b>	6.21	418	518, 552, 592, 648	660, 724	0.12	9.28 (0.93)
<b>3</b>	6.17	416	550, 590	612, 657	0.01	1.22 (1.03)
<b>4</b>	6.02	412	526, 560 (sh)	—	—	—

**Fig. 2.** UV-vis spectra of bisporphyrins **2** (solid), **3** (dashes) and **4** (dots) in dichloromethane**Fig. 3.** Fluorescence spectra of H<sub>2</sub>TPP (solid), ZnTPP (dashes), bisporphyrins **2** (dots) and **3** (dash-dot) in dichloromethane

$\lambda_{\text{emission}}$  for **2** vs. H<sub>2</sub>TPP shows little variation in most of the solvents studied, with a slight increase of the quantum yield ( $\Phi_{\text{F}}$ ). In comparison with ZnTPP, the  $\lambda_{\text{emission}}$  of **3** shows a slight red shift (to 612 and 657 nm) in most solvents studied. These observations are in agreement with the absorption changes, and indicate little interaction between the two porphyrin chromophores in **2** and **3**.

The fluorescence decay signals and fitted lines are presented in Table 1 and Fig. 4. The excited lifetimes

**Fig. 4.** The excited state lifetime of bisporphyrins **2** (dots) and **3** (solid) in dichloromethane measured with time-correlated single photon counting method fitting with one exponential

of bisporphyrins **2** and **3** were obtained by an interactive nonlinear deconvolution fitting procedure. The fitted fluorescence lifetime data for **2** and **3** are similar to the corresponding monoporphyrins (H<sub>2</sub>TPP and ZnTPP), respectively. In comparison to **2**, bisporphyrin **3** exhibits a large decrease of the fluorescence lifetime, similar to the literature result [26], which may be attributed to the heavy atom effect of zinc(II) metal ions. In addition, the lifetime decays are all monoexponential, indicating that only one species is fluorescing. This similarity indicates that the two porphyrin chromophores in both **2** and **3** have few interactions, and is consistent with most reported 5,17-substituted derivatives of coneshaped calix[4]arenes when the open conformation is adapted [27].

The solvent effect on the absorption spectra of these bisporphyrins was also studied and the results are summarized in Table 2. Polar protic solvents, such as methanol and ethanol, cause a blue shift (by 8–9 nm) of the Soret band for **2** versus H<sub>2</sub>TPP; on the other hand, polar aprotic solvents, such as DMSO and THF lead to a red shift (by 6–12 nm) of the Soret band for **3** vs. ZnTPP. The increased polarity of the solvent leads to the increased polarization forces between the solvent and the absorber (porphyrin), which lowers the energy levels of both the excited and unexcited states for  $\pi\text{-}\pi^*$  transitions. Since this effect is greater for the excited state, the energy

**Table 2.** UV-vis and fluorescence spectra of bisporphyrins **2** and **3** in various solvents

Solvent	Compounds	$\lambda_{\text{max}}^{\text{abs}}$ , nm	log $\epsilon$	$\lambda_{\text{max}}^{\text{em}}$ , nm	$\Phi_{\text{F}}^{\text{a}}$	Solvent	Compounds	$\lambda_{\text{max}}^{\text{abs}}$ , nm	log $\epsilon$	$\lambda_{\text{max}}^{\text{em}}$ , nm	$\Phi_{\text{F}}^{\text{a}}$
acetonitrile	H <sub>2</sub> TPP	413	5.56	656, 718	0.19	diethyl ether	H <sub>2</sub> TPP	414	5.56	654, 718	0.18
	<b>2</b>	404	5.74	657, 721	0.29		<b>2</b>	416	6.05	659, 722	0.12
	ZnTPP	423	5.83	610, 660	0.03		ZnTPP	419	5.83	608, 656	0.02
	<b>3</b>	418	6.10	614, 664	0.01		<b>3</b>	418	6.10	616, 664	0.03
methanol	H <sub>2</sub> TPP	412	5.51	654, 718	0.21	methylene chloride	H <sub>2</sub> TPP	417	5.34	656, 720	0.13
	<b>2</b>	404	5.49	658, 721	0.35		<b>2</b>	418	6.21	660, 724	0.12
	ZnTPP	419	5.87	606, 658	0.02		ZnTPP	422	5.67	602, 650	0.04
	<b>3</b>	416	6.09	614, 663	<0.01		<b>3</b>	416	6.17	612, 657	0.01
ethanol	H <sub>2</sub> TPP	413	5.62	654, 718	0.18	chloroform	H <sub>2</sub> TPP	418	5.61	658, 720	0.08
	<b>2</b>	404	5.77	659, 723	0.25		<b>2</b>	418	6.25	661, 724	0.09
	ZnTPP	420	5.88	608, 658	0.03		ZnTPP	421	5.83	604, 648	0.03
	<b>3</b>	422	6.05	615, 664	<0.01		<b>3</b>	416	6.17	611, 655	0.01
DMSO	H <sub>2</sub> TPP	418	5.57	656, 718	0.19	toluene	H <sub>2</sub> TPP	418	5.60	658, 720	0.09
	<b>2</b>	418	5.96	658, 723	0.18		<b>2</b>	420	6.26	659, 722	0.12
	ZnTPP	427	5.90	612, 664	0.04		ZnTPP	420	5.82	604, 650	0.03
	<b>3</b>	428	6.23	615, 662	<0.01		<b>3</b>	418	6.12	612, 655	0.04
THF	H <sub>2</sub> TPP	416	5.55	658, 720	0.02	carbon tetrachloride	H <sub>2</sub> TPP	419	5.56	658, 722	0.06
	<b>2</b>	416	6.27	659, 724	0.12		<b>2</b>	420	6.23	662, 725	0.12
	ZnTPP	423	5.91	610, 658	<0.01		ZnTPP	421	5.86	606, 646	0.04
	<b>3</b>	422	6.23	615, 663	0.02		<b>3</b>	418	6.19	615, 657	0.03
ethyl acetate	H <sub>2</sub> TPP	414	5.59	654, 718	0.13	cyclohexane	H <sub>2</sub> TPP	416	5.55	658, 720	0.11
	<b>2</b>	414	6.17	657, 722	0.12		<b>2</b>	408	5.87	661, 725	0.16
	ZnTPP	419	5.76	606, 656	0.02		ZnTPP	424	5.91	602, 644	0.03
	<b>3</b>	420	6.19	612, 661	0.02		<b>3</b>	416	6.06	619, 666	0.03

<sup>a</sup> Room temperature, excited at 500 nm. The reference for quantum yield is H<sub>2</sub>TPP in DMF 0.11 [20] and ZnTPP in toluene 0.03 [21].

difference between the excited and unexcited states is slightly reduced, resulting in a small red shift of the Soret band as observed in **3**. On the other hand, the observed small blue shift for **2** due to the polarity change of the solvent might have arisen from the conformational changes of calix[4]arene, as described in literature [28–29]. For example, based on X-ray structures, Love *et al.* have observed two different structural motifs of a calixpyrrole macrocycle in the presence of a protic solvent: a non-planar bowl-like conformation in ethanol and a Pacman-type conformation in water [29].

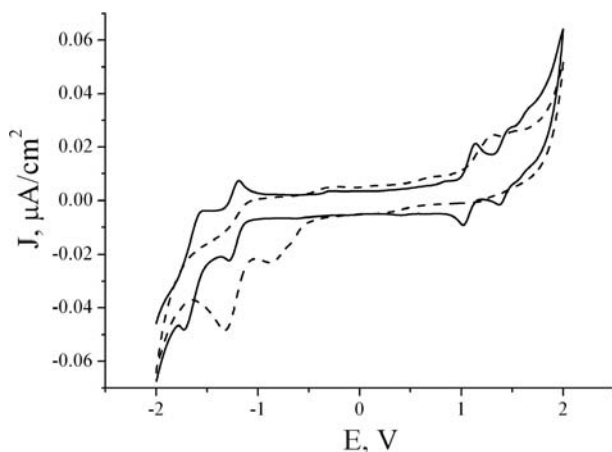
Since the aggregation of these bisporphyrins in solution may also bring about variation of the absorption spectra, to verify the metal ion effect on the spectral changes of these molecules, we also investigated the relationship between the absorption spectra and the concentration of these bisporphyrins. The absorption maxima were found

to be independent of the concentration of these bisporphyrins (typically 10<sup>-4</sup>–10<sup>-6</sup> M). The linear relationship between the absorption intensity and the concentration of these bisporphyrins indicates no anomalous behavior associated to aggregation effects, as previously described for cofacial bisporphyrins [2, 6, 7c].

The cyclic voltammetric (CV) data for bisporphyrin **2**, **3** and **4** are shown in Table 3. All cyclic voltammograms are similar in shape and yielded three or four peaks, depending on the presence and nature of the metal ions at the center of the porphyrin macrocycles. The electron transfers are in all cases diffusion-controlled and yielded well-defined current-voltage curves with the theoretical peak separation for a one-electron transfer. H<sub>2</sub>TPP is used as a reference, giving two redox peaks (-1.01 V and -1.32 V) and two oxidation peaks (1.20 V and 1.54 V) corresponding to the macrocycle-centered reduction and

**Table 3.** Cyclic voltammograms (CV) data of **2**, **3** and **4** in dichloromethane under pure N<sub>2</sub> atmosphere

Compound	$E_{ox}$ , V vs Ag/AgCl		$E_{re}$ , V vs Ag/AgCl	
H <sub>2</sub> TPP	1.54	1.20	-1.01	-1.32
ZnTPP	1.37	0.89	-1.38	-1.59
CuTPP	1.42	1.08	-1.23	-1.64
<b>2</b>	1.33	1.20	-1.06	-1.45
<b>3</b>	1.32	0.81	-1.43	-1.51
<b>4</b>	1.62	1.27	-0.97	-1.50

**Fig. 5.** Cyclic Voltammograms of  $1 \times 10^{-3}$  M CuTPP (solid) and  $1 \times 10^{-3}$  M bisporphyrin **4** (dashes) in dry dichloromethane. Trihexyl(tetradecyl)phosphonium hexafluorophosphate as the supporting electrolyte at a concentration of 0.1 M, glassy carbon electrode (GCE) as a working electrode, and scan rate at 60 mV.s<sup>-1</sup>

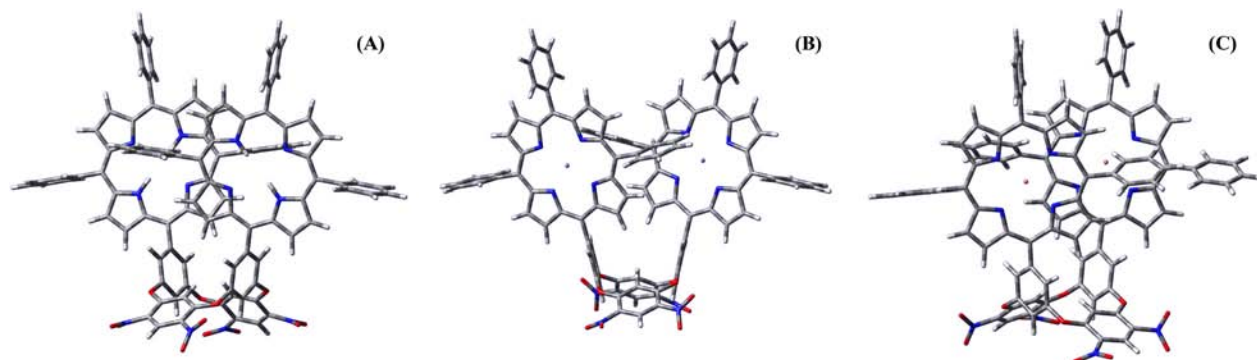
oxidation reactions, which is consistent with previous reported values [30]. The comparison of the CV data of **2** vs. H<sub>2</sub>TPP shows little variation: two redox peaks (-1.06 V and -1.45 V) and two oxidation peaks (1.20 V and 1.33 V). All four reactions were diffusion-controlled and, in agreement with previous electrochemical results, the potential difference between anion and cation radical formation (2.26 V) is  $2.25 \pm 0.15$  V [31]. This result is consistent with the photophysical changes described

above and indicates little electronic interaction between the two porphyrin macrocycles. The comparison of the CV data for **3** vs. ZnTPP also shows little variation and indicates little electronic interactions between the two porphyrin macrocycles. The voltammogram for **4** was similar in shape and form to that of **3**, and the  $E_{1/2}$  is proportional to the electronegativity of the central metal ions as observed for metalloporphyrins with stable two-valent central metal ions (Zn and Cu) [32]. The overlaid CV spectra for **4** and CuTPP was shown in Fig. 5, which indicates the electronic communication between the two porphyrin macrocycles and is consistent with the photophysical changes described above.

We further investigated the distance between the two porphyrin macrocycles based on the HF/CEP-31G calculation results [18]. The *ab initio* HF/CEP-31g optimized structures of bisporphyrins **2**, **3** and **4** are shown in Fig. 6. The optimized structure for the metal-free bisporphyrin **2** was in agreement with the X-ray structure of this molecule, with the distance between two porphyrin macrocycles at 8.471 Å. In comparison with complex **2**, a slight increase of the distance was observed in bisporphyrin **3** (8.557 Å) after the insertion of Zn<sup>2+</sup> into the porphyrin macrocycles, while a large decrease of the distance was observed in bisporphyrin **4** (7.108 Å) after the insertion of Cu<sup>2+</sup>. The short distance observed in bisporphyrin **4** may account for the enhanced electronic communication between the two porphyrin macrocycles, which is in consistency with the photophysical changes and CVs described above.

## CONCLUSION

We report the syntheses of a series of cofacial homobimetallic bisporphyrins, their photophysical and electronic properties, and HF/CEP-31G computational results, along with those of a previously reported metal-free bisporphyrin. We observed little electronic interaction between the two porphyrin macrocycles in the free-base and biszinc(II) complexes **2** and **3**, while enhanced electronic interactions were observed between the two porphyrin macrocycles in **4** bearing two copper(II) ions.

**Fig. 6.** Tube models of the *ab initio* HF/CEP-31G optimized structures of bisporphyrins (A) **2**, (B) **3** and (C) **4**

## Acknowledgements

This work is supported by the National Nature Science Foundation of China (Grants 20802002, 20902004 and 20875002), Anhui Province (Grants 090416221 and KJ2009A130) and the United States National Science Foundation (Grant CHE-0911629).

## REFERENCES

1. a) Choi MS, Yamazaki T, Yamazaki I and Aida T. *Angew. Chem. Int. Ed.* 2004; **43**: 150. b) Kuramochi Y, Satake A and Kobuke Y. *J. Am. Chem. Soc.* 2004; **126**: 8668.
2. Faure S, Stern C, Guillard R and Harvey PD. *J. Am. Chem. Soc.* 2004; **126**: 1253.
3. Chang CJ, Loh ZH, Shi C, Anson FC and Nocera DG. *J. Am. Chem. Soc.* 2004; **126**: 10013.
4. a) Collman JP, Wagenknecht PS and Hutchison JE. *Angew. Chem. Int. Ed. Eng.* 1994; **33**: 1537. b) Chng LL, Chang CJ and Nocera DG. *J. Org. Chem.* 2003; **68**: 4075. c) Fletcher JT and Therien MJ. *J. Am. Chem. Soc.* 2000; **122**: 12393. d) Deng Y, Chang CJ and Nocera DG. *J. Am. Chem. Soc.* 2000; **122**: 410. e) Clement TE, Nurco DJ and Smith KM. *Inorg. Chem.* 1998; **37**: 1150.
5. Harvey PD, Stern C, Gros CP and Guillard R. *Coord. Chem. Rev.* 2007; **251**: 401.
6. Bolze F, Gros CP, Drouin M, Espinosa E, Harvey PD and Guillard R. *J. Organomet. Chem.* 2002; **643–644**: 89.
7. a) Harvey PD, Proulx N, Martin G, Drouin M, Nurco DJ, Smith KM, Bolze F, Gros CP and Guillard R. *Inorg. Chem.* 2001; **40**: 4134. b) Bolze F, Drouin M, Harvey PD, Gros CP, Espinosa E and Guillard R. *J. Porphyrins Phthalocyanines* 2003; **7**: 474. c) Bolze F, Gros CP, Harvey PD and Guillard R. *J. Porphyrins Phthalocyanines* 2001; **5**: 569.
8. Faure S, Stern C, Espinosa E, Douville J, Guillard R and Harvey PD. *Chem. Eur. J.* 2005; **11**: 3469.
9. a) Chang CJ, Baker EA, Pistorio BJ, Deng Y, Loh ZH, Miller SE, Carpenter SD and Nocera DG. *Inorg. Chem.* 2002; **41**: 3102. b) Chang CJ, Deng Y, Heyduk AF, Chang CK and Nocera DG. *Inorg. Chem.* 2000; **39**: 959.
10. Deng Y, Chang CJ and Nocera D. G. *J. Am. Chem. Soc.* 2000; **122**: 410.
11. Faure S, Stern C, Guillard R and Harvey PD. *Inorg. Chem.* 2005; **44**: 9232.
12. a) Khoury RG, Jaquinod L, Aoyagi K, Olmstead MM, Fisher AJ and Smith KM. *Angew. Chem. Int. Ed.* 1997; **36**, 2497. b) Jokic D, Asfari Z and Weiss J. *Org. Lett.* 2002; **4**: 2129. c) Tremblay-Morin JP, Faure S, Samar D, Stern C, Guillard R and Harvey PD. *Inorg. Chem.* 2005; **44**: 2836. d) Baldini L, Ballester P, Casnati A, Gomila RM, Hunter CA, Sansone F and Ungaro R. *J. Am. Chem. Soc.* 2003; **125**: 14181. e) Di Costanzo L, Geremia S, Randaccio L, Purrello R, Lauceri R, Sciotto D, Gulino FG and Pavone V. *Angew. Chem. Int. Ed.* 2001; **40**: 4245. f) Collman JP, Hutchinson JE, Lopez MA, Tabard A, Guillard R, Seok WK, Ibers JA and L'Her M. *J. Am. Chem. Soc.* 1992; **114**: 9869. g) Chang CK and Abdalalmuhdi I. *J. Org. Chem.* 1983; **48**: 5388.
13. Sanders JKM. In *The Porphyrin Handbook*, Vol. 3, Kadish KM, Smith KM and Guillard R. (Eds.) Academic Press: San Diego, CA, 2000; pp 347.
14. a) Katz JL, Feldman MB and Conry RR. *Org. Lett.* 2005; **7**: 91. b) Wang MX and Yang HB. *J. Am. Chem. Soc.* 2004; **126**: 15412.
15. a) Harvey PD. *Coord. Chem. Rev.* 2002; **233–234**: 289. b) Harvey PD. *J. Inorg. Organomet. Poly.* 2004; **14**: 211.
16. Hao EH, Fronczek FR and Vicente MGH. *J. Org. Chem.* 2006; **71**: 1233.
17. Tanaka T, Endo K and Aoyama Y. *Bull. Chem. Soc. Jpn.* 2001; **74**: 907.
18. a) Ghosh A. *Acc. Chem. Res.* 1998; **31**: 189. b) Chitta R, Rogers LM, Wanklyn A, Karr PA, Kahol PK, Zandler ME and D'Souza F. *Inorg. Chem.* 2004; **43**: 6969. c) Almlöf J, Fischer TH, Gassman PG, Ghosh A and Häser M. *J. Phys. Chem.* 1993; **97**: 10964. d) Piqueras MC and Rohlfling CM. *Theor. Chem. Acc.* 1997; **97**: 81.
19. *Molecular Fluorescence: Principles and Applications*, Valeur B. (Ed.) Wiley-VCH: Weinheim, Germany, 2002.
20. Seybold PG and Gouterman MP. *J. Mol. Spectr.* 1969; **31**: 1.
21. Strachan JP, Gentemann S, Seth J, Kalsbeck WA, Lindsey JS, Holten D and Bocian DF. *J. Am. Chem. Soc.* 1997; **119**: 11191.
22. Williams ATR, Winfield SA and Miller JN. *Analyst* 1983; **108**: 1067.
23. Olmsted J. *J. Phys. Chem.* 1979; **83**: 2581.
24. a) Harvey PD. In *The Porphyrin Handbook*, Vol. 18, Kadish KM, Smith KM and Guillard R. (Eds.) Academic Press: San Diego, 2003; pp 63. b) Collman JP, Wagenknecht PS and Hutchinson JE. *Angew. Chem. Int. Ed.* 1994; **33**: 1537.
25. a) Gouterman M, Holten D and Lieberman E. *Chem. Phys.* 1977; **25**: 139. b) Chang CK. *J. Heterocycl. Chem.* 1977; **14**: 1285.
26. a) Harvey PD. *Coord. Chem. Rev.* 2002; **233**: 289. b) Gagnon J, Vézina M, Drouin M and Harvey PD. *Can. J. Chem.* 2001; **79**: 1439.
27. Tremblay-Morin JP, Faure S, Samar D, Stern C, Guillard R and Harvey PD. *Inorg. Chem.* 2005; **44**: 2836.

28. a) Ikeda A and Shinkai S. *Chem. Rev.* 1997; **97**: 1713. b) Fletcher NC, Ward MD, Encinas S, Armaroli N, Flamigni L and Barigelletti F. *Chem. Commun.* 1999; 2089.
29. Love JB. *Chem. Commun.* 2009; 3154.
30. Kadish KM and Morrison MM. *J. Am. Chem. Soc.* 1976; **98**: 3326.
31. a) Fuhrhop JH, Kadish KM and Davis DG. *J. Am. Chem. Soc.* 1973; **95**: 5140. b) Kadish KM, Davis DG and Fuhrhop JH. *Angew. Chem. Int. Ed.* 1972; **11**: 1014.
32. a) Fuhrhop JH and Mauzerall D. *J. Am. Chem. Soc.* 1968; **90**: 3875. b) Fuhrhop JH and Mauzerall D. *J. Am. Chem. Soc.* 1969; **91**: 4174.

Copyright of the works in this Journal is vested with World Scientific Publishing. The article is allowed for individual use only and may not be copied, further disseminated, or hosted on any other third party website or repository without the copyright holder's written permission.